EPJ manuscript No.
(will be inserted by the editor)

Dynamics of intramolecular recognition: base-pairing in DNA/RNA near and far from equilibrium

Ralf Bundschuh[1] and Ulrich Gerland[2]

[1] Department of Physics, The Ohio State University, Columbus, Ohio 43210-1117, USA
[2] Arnold-Sommerfeld Center for Theoretical Physics and Center for Nanoscience (CeNS), LMU München, Theresienstrasse 37, 80333 München, Germany

January 30, 2006

Abstract. The physics of the base-pairing interaction in DNA and RNA molecules plays a fundamental role in biology. Past experimental and theoretical research has led to a fairly complete and quantitative understanding of the equilibrium properties such as the different phases, the melting behavior, and the response to slow stretching. The non-equilibrium behavior is even richer than might be expected on the basis of the thermodynamics. However, the non-equilibrium behavior is also far less understood. Here, we review different theoretical approaches to the study of base-pairing thermodynamics and kinetics, and illustrate the rich phenomenology with several examples that use these approaches.

PACS. 87.15.Cc Folding and sequence analysis – 87.15.He Dynamics and conformational changes – 87.14.Gg DNA, RNA

1 Introduction

The base-pairing interaction in DNA and RNA is a prototypic example of molecular recognition in biology. On the one hand, base-pairing is remarkably simple, with a relatively small and well-defined set of interactions between the four different chemical monomers of these heteropolymers. On the other hand, this interaction gives rise to the amazingly complex physical and biochemical properties of DNA and RNA, which appear to be exploited by nature in almost every possible way [1]. It has long been appreciated that DNA is uniquely suited for reliably storing genetic information while keeping it accessible for readout (transcription), copying (DNA replication), cut & paste (DNA recombination), and repair. In contrast, the role of RNA in molecular biology was long seen merely as messenger of genetic information. However, a series of discoveries in the past 20 years revealed important enzymatic and regulatory functions that moved RNA into the spotlight today [2]. Here, our focus is on the physical properties of DNA and RNA emerging from the base-pairing interaction, and their biological ramifications.

Clearly, the biochemical properties of DNA and RNA are equally important as the physical properties and sometimes essential to understand the function, as in the case of RNA enzymes [3]. However, we will argue here that much can be learned already from the thermodynamics and kinetics of base-pairing. To this end, it is instructive to consider a few biological examples, which illustrate the functional role of these physical properties. One well-documented case is the heat-shock response of *E. coli*, where the base-pairing pattern of a messenger RNA (mRNA) acts as a molecular thermosensor [4]: When the bacterium is exposed to a heat shock (e.g. temperature rise to 42^oC), it quickly starts producing a set of heat shock proteins. The trigger for this emergency response is the upregulation of a single protein concentration (the sigma factor σ^{32}), which controls the production of all heat shock proteins. At normal temperatures, the mRNA of σ^{32} has a stable base-pairing pattern in the vicinity of the translation start, thereby masking the ribosome binding site and suppressing translation initiation. However, at an elevated temperature, the secondary structure melts so that the ribosome binding site becomes accessible and the mRNA is translated at a high rate. Thus, in this example the thermodynamics of base-pairing provides an essential function.

Similarly, there are examples where base-pairing kinetics plays a functional role [5–7]. One well-studied case occurs in the RNA bacteriophage MS2, a virus with an RNA genome that infects bacteria such as *E. coli* [5]. Since the genome also acts as mRNA, any control of gene expression must be at the level of translation. Indeed, the expression of its small set of four genes is controlled to assure proper timing and quantities of the protein products which guide MS2 reproduction. In particular, the maturation gene must be expressed only in a short time window after MS2 is synthesized in the invaded bacterium. Nature's solution is a slow-folding secondary structure at the translation start site [5]: When the secondary structure has correctly folded, it is thermodynamically stable and

shuts down translation by masking the ribosome binding site. However, directly after synthesis, the structure has not yet formed and translation takes place. The structure is slow-folding because of an alternative base-pairing pattern that acts as a kinetic trap.

The thermodynamics and kinetics of base-pairing is evidently fundamental to the ubiquitous problem of RNA folding. In many cases, the function of RNA molecules requires a well-defined three-dimensional (so-called tertiary) structure, which involves other interactions besides base-pairing [8]. However, the formation of secondary structure (i.e., base-pairing) is not only a prerequisite for the formation of tertiary structure, it can also be studied independently, since tertiary interactions are dependent on the presence of divalent Mg ions, which can be removed in experiments. Indeed, due to the ongoing advances in single molecule techniques, the dynamics of RNA folding is being probed in increasing detail, providing possibilities for a fruitful interplay between theory and experiment [9–11].

Here, we give a perspective from the viewpoint of theory. The discussion is organized into two main sections. Section 2 is dedicated to the thermodynamics of base-pairing while Section 3 focuses on the kinetics of base-pairing. Each of these two main sections starts with a presentation of the main concepts and methods used to describe the respective phenomena. Then, these approaches are illustrated using specific examples. Given the breadth of the field we did not attempt to exhaustively cover all the interesting physics of base-pairing but instead picked examples that illustrate our point and that certainly are a reflection of our own taste. Section 4 concludes the discussion by summarizing our main point again.

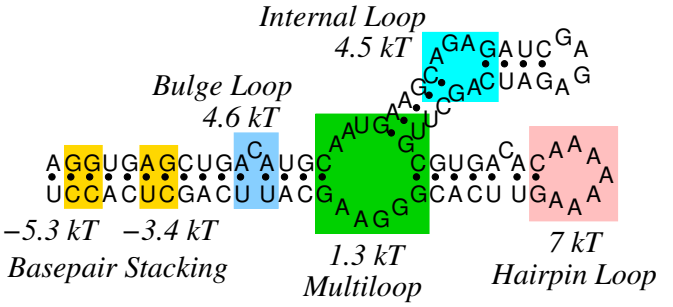

Fig. 1. Representation of a base-pairing configuration and different types of loops in a nucleic acid molecule. In a realistic energy model, each base-pair stacking and each loop is assigned an effective free energy which depends on the identities of the bases and the type and length of a loop. The total free energy of a base-pairing configuration is then approximated as the sum of the individual free energy contributions.

2 Equilibrium properties

Base-pairing in nucleic acids is the formation of hydrogen bonds between the individual monomers of a DNA or RNA molecule. These monomers are guanine (G), cytosine (C), adenine (A), and tyrosine (T) in the case of DNA. In RNA, tyrosine is replaced by the base uracil (U). The most frequent and most stable form of base-pairing are the Watson-Crick base-pairs G–C and A–T (or A–U in the case of RNA). However, also the wobble base-pair G–U frequently occurs in natural RNA structures. Other types of base-pairs are less stable but nevertheless occur occasionally, especially if they are stabilized by neighboring Watson-Crick base-pairs.

2.1 Energetics of base-pairing

Before embarking on a discussion of the physics that base-pairing in DNA and RNA brings about, we want to give an overview of the microscopic models underlying the description of these emergent properties of DNA and RNA. Since we are looking for an understanding of the thermodynamics (and later the kinetics) of DNA and RNA from the base-pairing level, "microscopic" means that we associate an individual state of the molecule with every possible base-pairing pattern. In a double-stranded DNA molecule each base has its designated "partner base" to which it can either be bound or not. Thus, a state can naturally be described by assigning an Ising variable to each base-pair along the chain the two states of which are "closed" and "open". For RNA molecules (or single-stranded DNA molecules) although each base can still bind to only one binding partner at a time, each base has the possibility to form this pair with many different potential binding partners. In this case a state of the molecule is more conveniently described by the list of the base-pairs that have formed. A more visual representation of such a state is by a diagram of the kind shown in Fig. 1.

Once the states of the statistical mechanical description are chosen, each of them has to be associated with an energy in order to model the thermodynamics of the system. For each base-pairing configuration there are many different true microstates of the system such as different spatial configurations of the molecule and different configurations of the surrounding water molecules and counter ions. Thus, the energy associated with a base-pairing configuration is actually an effective free energy which is obtained by integrating out all degrees of freedom of the molecule and the solvent while the base-pairing configuration is held fixed.

Since it is currently not possible to derive these effective free energies from first principles, one resorts to a variety of different energy models. The crudest effective free energy model simply assigns a constant effective binding energy to every closed base-pair, i.e., the effective free energy of a state is proportional to the number of base-pairs in this state. This model, which we will refer to as the "uniform pairing" energy model, is useful if qualitative features of base-pairing are studied. Its simplicity lends itself to analytical approaches. If one is interested in qualitative effects of sequence heterogeneity, a simple extension of this model still assigns an individual contribution to the total effective free energy to each base-pair

but uses different energies depending on the type of the base-pair. This reflects the fact that G–C base-pairs are more stable than A–T base-pairs which in turn are more stable than the G–U base-pairs. We will refer to this model as the "sequence-dependent pairing" energy model.

While the above free energy models are very useful in order to study qualitative features of the physics of base-pairing, they lack many of the details that govern the more quantitative aspects of base-pairing. One important detail is that the largest stabilizing contribution to the effective binding energy of a base-pair actually does not come from one base-pair alone but from the *stacking* of two neighboring base-pairs. Thus, more realistic energy models attribute their additive contributions to the total effective free energy not to the base-pairs but to the stacks of consecutive base-pairs, resulting in the "uniform stacking" and the "sequence-dependent stacking" energy model respectively depending on the fact if this stacking energy depends on the identity of the four bases involved in the two base-pairs or not. For this sequence-dependent stacking energy model the stacking energies for all possible combinations of two consecutive base-pairs have been measured extensively for DNA [12] as well as for RNA [13].

Another aspect that makes effective free energy models more realistic is the way in which they take the entropy resulting from the spatial degrees of freedom of the backbone into account. Each base-pairing imposes further constraints on these spatial degrees of freedom. After integrating the spatial degrees of freedom out, these constraints translate into a repulsive entropic contribution to the effective free energy. The extensive part of this entropy (i.e., the reduction in entropy per base due to the binding of a base-pair) can be taken into account in the effective binding energy for each base-pair or base stacking and merely changes the numerical values of the binding energy parameters in the models discussed above. However, there is an additional loss of entropy upon binding of a base-pair associated with the unbound bases which without the formation of this base-pair would have fluctuated freely but are forced to form a *loop* (see Fig. 1) once the base-pair is closed. The asymptotic (large loop length) form of this loop entropy (in units of k_B) is $c \log \ell$ where ℓ is the length of the loop and c is some prefactor. For Gaussian chains in three dimensions without self-avoidance this prefactor is $c = 3/2$ [14] but self-avoidance increases this value [15] and there is some debate as to by how much [16]. If this effect is taken into account in an energy model we will indicate this by appending the term "with loop entropy" to its name.

The most detailed free energy model still starts from the assumption that the total effective free energy of a state is the sum of the (sequence-dependent) stacking free energies of all the stacking pairs and the loop free energies of all loops of the state (see Fig. 1). While this assumption is known to be not strictly true (sequences that only differ in the order in which stackings appear should have the exact same binding free energy according to this model but are experimentally known to not have the same binding free energy [12]) the assumption is still good enough to produce practically useful quantitative results such as the prediction of RNA secondary structures from sequence alone. Instead of using the simple logarithmic free energy cost for loops realistic models acknowledge that for short loops effects such as bending energy and partial stacking of unpaired bases contribute to the effective loop free energy. Thus, the effective free energy of loops is allowed to depend on the length of the loop, the type of the loop (see Fig. 1), and on the identities of the bases in the base-pairs closing the loop. This results in thousands of free energy parameters that describe such a model. All these parameters are measured by melting small DNA and RNA molecules with well-defined structures, recording their melting thermodynamics quantitatively, extracting their total effective free energies of binding, and reconstructing the contributions of the individual elements of the structures using the additive assumption [17]. We will refer to this energy model short as the "realistic" energy model.

2.2 DNA thermodynamics

2.2.1 Experimental observations

The thermodynamics of double-stranded DNA is a well-studied subject. Experimentally, the most obvious phenomenon is a melting transition as the temperature of a solution of double-stranded DNA is raised from physiological temperatures to about 80^oC. This melting transition can, e.g., be observed by measuring chromatic dichroism which is sensitive to the amount of helical (double-stranded) regions in the molecules. More quantitative information such as binding energies can be obtained from melting DNA or RNA in calorimeters. In this setup a peak in the heat capacity is the signature of the melting transition.

At first sight the radical change in behavior from a double stranded form to a single stranded form over a temperature range that is only some 10% of the absolute temperature at which it happens is surprising. It turns out to be driven by a subtle balance between entropy and energy. As discussed above, the effective free energy per base-pair is the difference between the chemical binding energy and the loss of entropy associated with the formation of a base-pair. At physiological temperatures both these quantities are on the order of $10kT$ [13]. Thus, they nearly cancel leaving a difference of a few kT in favor of the chemical binding energy. Thus, upon a relatively small change in temperature the balance in this cancellation of two large terms tips. This change in sign of the effective binding energy per base is what drives the melting transition. This marginal stability at physiological conditions is certainly not a coincidence but rather dictated by the fact that these molecules on the one hand must be stable enough to store genomic information while on the other hand many biological processes require the temporary local "melting" of DNA or RNA helices.

2.2.2 Modeling approaches

As discussed above, thermodynamics of double-stranded DNA can be described by a set of Ising variables. The uniform pairing energy model translates in the magnetic analogy into a set of non-interacting spins coupled to an external magnetic field. Thus, the magnetization (fraction of helical regions) is a smooth function of temperature without any phase transitions or even peaks in the heat capacity. A more successful model of DNA melting uses the uniform stacking energy model [18]. The stacking interaction between two neighboring base-pairs translates directly into the usual Ising interaction between neighboring spins. Thus, this model maps directly onto the one-dimensional Ising model which shows cooperativity and thus a peak in the heat capacity. However, the melting is still not associated with a phase transition which is to be expected since the Mermin-Wagner theorem [19] allows phase transitions in one-dimensional systems only in the presence of long-range interactions. Such long-range interaction is present in the uniform stacking energy model with loop entropy which is called the Poland-Scheraga model [14, 20] for double-stranded DNA or in the Peyrard-Bishop model [21] that explicitly takes into account some of the spatial degrees of freedom instead of including them into an effective loop entropy cost. Indeed, these models predict true phase transitions. In the Poland-Scheraga model, the order of this phase transition depends on the prefactor c of the logarithmic loop free energy. The transition is second order for $c < 2$ and first order for $c > 2$ [15]. While it was a major success that the Poland-Scheraga theory obtained a phase transition at all, mechanisms that explain the experimentally observed first order nature of this phase transition are still very controversially discussed [16, 22–27].

While the partition function for the uniform models such as the Poland-Scheraga model can be calculated exactly analytically, the inclusion of sequence-dependence requires either approximative [28] or numerical [29] methods. Conveniently, even for the very detailed realistic energy model it is possible to calculate the partition function of a double-stranded DNA molecule of arbitrary sequence with a time complexity that is quadratic in the length N of the sequence. This is achieved by calculating the partition function of all base-pairs $1, \ldots, i$ under the constraint that base-pair i is closed. If we denote this quantity by Z_i, we find that either base-pair i is the only base-pair among $1, \ldots, i$ that is closed or there must be another base-pair j which is the last base-pair before i that is closed. This yields the recursion relation

$$Z_i = 1 + q_i Z_{i-1} + \sum_{j=1}^{i-2} l(i,j) Z_j \qquad (1)$$

where q_i is the Boltzmann factor which corresponds to the stacking energy between the base-pair $i-1$ and the base-pair i while $l(i,j)$ is the Boltzmann factor for a loop of unbound base-pairs flanked by the closed base-pairs j and i. Since either one base-pair is the last closed base-pair or none of the base-pairs are closed, the total partition function of the molecule then becomes $Z = 1 + \sum_{i=1}^{N} Z_i$. This approach to the thermodynamics of DNA melting has been widely used to quantitatively model DNA melting [30–34].

2.3 RNA thermodynamics

2.3.1 Theoretical framework

Studying the thermodynamics of RNA or single-stranded DNA is more complicated than that of double-stranded DNA since there is more than one binding partner for each base. Usually, one restricts the space of all allowed states to states without pseudo-knots [8], i.e., if (i,j) and (k,l) are base-pairs with $i < k$, they have to either be independent ($i < j < k < l$) or nested ($i < k < l < j$). This restriction is justified because pseudo-knots with long helices require the end of the molecule to be threaded through an already existing loop in order to be formed which is kinetically very difficult (see Fig. 2) while short pseudo-knots do not contribute much to the overall free energy and thus their omission is not too bad an approximation. It should be said however, that for several biologically important RNAs pseudo-knots are crucial for their biological function.

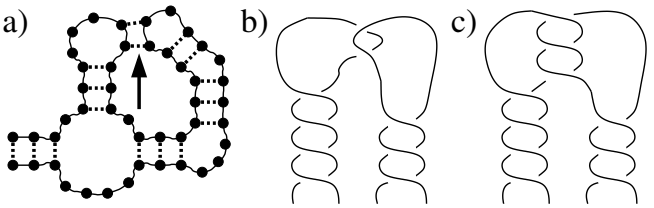

Fig. 2. Pseudo-knots in RNA structures: The base-pairings indicated by the arrow in (a) create a pseudo-knot. We exclude such configurations in our definition of secondary structures: The short pseudo-knots (called "kissing hairpins") as shown in (b) do not contribute much to the total binding energy, and the long ones shown in (c) are kinetically forbidden since the double helical structure would require threading one end of the molecule through its loops many times.

If one excludes pseudo-knots, there is again a recursive approach to calculating the complete partition function of an RNA molecule of a given sequence in polynomial time in the length N of the sequence [35–38]. For the simplest energy model that assigns only an effective binding energy to each base-pair (which may depend on the identity of the two bases involved) and no free energy to the loops, this recursion can be written in terms of the partition function $Z_{i,j}$ for the subsequence from base i to base j. The recursion is obtained by realizing that base j can either be unbound or bound to exactly one of the bases

$i \dots j-1$ which yields [39]

$$Z_{i,j} = Z_{i,j-1} + \sum_{k=i}^{j-1} Z_{i,k-1} q_{k,j} Z_{k+1,j-1} \qquad (2)$$

where $q_{k,j}$ is the Boltzmann factor associated with the binding energy of the base-pair (k,j). The second term on the right hand side factorizes into the product of two partition functions because the no pseudo-knot constraint forbids any base-pairing between a base $i \dots k-1$ and a base $k+1, \dots j-1$. The partition function for the more realistic free energy model with stacking energies and loop entropies can be calculated by similar, but more complicated recursion equations. However, in order to still keep the $O(N^3)$ computational complexity some approximations to the loop free energies have to be made, specifically the cost of a multi-loop (a loop closed by more than two base-pairs) has to be assumed to be linear in its length and the number of closing base-pairs. Nevertheless, numerical tools like mfold [40], the Vienna package [41], and sfold [42], which rely on this approach are routinely and successfully used for the computational prediction of thermodynamic features of RNA secondary structures by biologists. However, for short RNA sequences even structure prediction with logarithmic multi-loop free energies is feasible due to its $O(N^4)$ complexity.

2.3.2 Phase diagram of RNA secondary structures

From a more physical point of view one can ask about the thermodynamic phase diagram of RNA base-pairing. In this quest Eq. (2) is a starting point both for numerical and analytical approaches. The melting "transition" has been studied in the uniform stacking energy model with loop entropy by de Gennes already nearly forty years ago [35]. This study, which assumes Gaussian statistics for the loop entropy, i.e., a prefactor of $c = 3/2$ of the loop entropy, comes to the conclusion that melting in this model is not a true phase transition although the cooperativity induced by stacking results in a pronounced peak in the heat capacity. However, melting becomes a true phase transition if the prefactor c is larger than 2.

A question that has been studied more recently is if sequence disorder induces a phase transition between a low-temperature glassy phase [43–52] where the thermodynamic ensemble of structures is dominated by one or a few base-pair configurations and a high-temperature "molten" phase where still most of the bases are paired but a very large number of base-pair configurations coexist (not to be confused with the "denatured" phase which describes the phase in which the bases do not form any pairs any more). In the sequence-dependent pairing energy model such a transition indeed exists [50]. However, it is not clear if this transition happens below the denaturation temperature in realistic energy models or if the real RNA molecule denatures before the "molten" phase of the base-pairing configurations is reached.

While these considerations apply to randomly chosen RNA sequences, the sequences of structural RNAs are certainly not random but are on the contrary designed such that the RNA folds preferentially into the "native" structure it needs to take in order to perform its biological function. Thus, the degree of sequence design or bias toward the native structure is another parameter the thermodynamics of RNA molecules depends on. If the bias is strong enough one would expect the molecule to go into a native phase no matter what phase it is in without the bias. This results in the phase diagram shown in Fig. 3. It remarkably resembles the phase diagram for proteins in its general topology (see, e.g., [53]). In this phase diagram the molten, native, and denatured phase as well as the melting transition [35], the molten-native transition [54] and the native-denatured transition [55] can be understood quantitatively. In contrast, there is still relatively little known analytically about the glass phase and the transitions into it except for its existence itself.

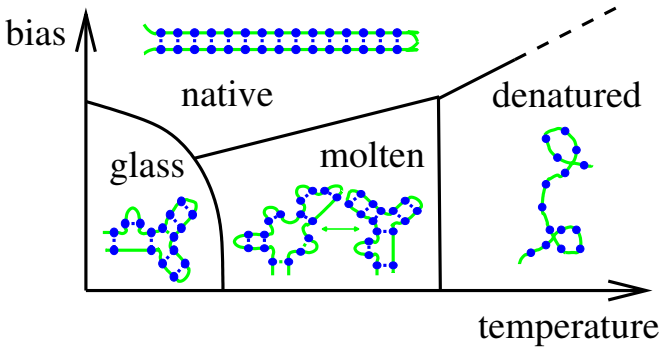

Fig. 3. Thermodynamic phase diagram of RNA base-pairing. Completely random RNA sequences (no bias) go from a glassy phase through a molten phase into a denatured phase as temperature is increased. As the sequence is more and more biased toward a specific "native" structure, the molecule enters the native phase where the native structure dominates at all temperatures.

An open question in RNA structure thermodynamics is the inclusion of pseudo-knots. Given that in many structural RNAs pseudo-knots are essential for the biological function it is an obvious question how to include pseudo-knots in quantitative analyses of RNA base-pairing configurations. There are several approaches to extend the thermodynamics framework described above to pseudo-knots [56–59]. Since including all pseudo-knots is known to be NP-complete [60], most of these approaches specify a certain sub-class of pseudo-knots and derive recursion equations of higher but still polynomial complexity than in the approach without pseudo-knots. However, all these approaches suffer from the fact that there is no obvious criterion which class of pseudo-knots is a good one to consider. An additional problem is that no good free energy parameters for pseudo-knotted configurations are available, which can be somewhat circumvented by trying to derive such parameters from more fundamental considerations of spatial entropy [57, 61].

2.3.3 Single molecule experiments

As single molecule experiments probing the base-pairing of nucleic acid molecules have appeared [9, 10, 62] the thermodynamic approach has been applied to these kinds of experiments as well [63–66]. This makes sense as long as the time scales probed in the experiments are longer than the time scales involved in the structural rearrangements of the RNA molecule. This is, e.g., the case in the early force-extension experiments on RNA [10] and single-stranded DNA [62]. In these experiments a short RNA molecule (50 bases) [10] or a very long single-stranded DNA molecule (50,000 bases) [62] were attached to macroscopic objects at both ends as shown in Fig. 4. As the

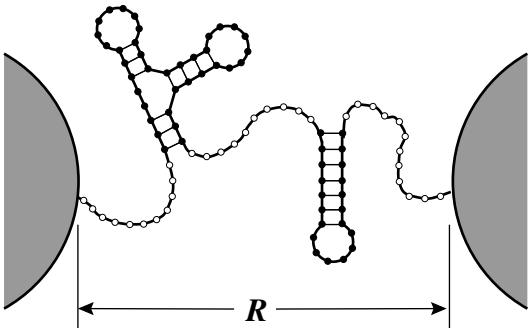

Fig. 4. Sketch of a force-extension experiment (from [64]). The two ends of an RNA molecule are connected to beads (not shown to scale). The force required to keep the molecule's ends at a given distance R is measured. For a given secondary structure this force is determined by the mechanical properties of the m externally accessible bases indicated by the open circles.

distance between these ends is slowly increased the force required to hold the molecule at a given distance is measured. The resulting force-extension curve reflects information about the base-pairing pattern of the molecule for very short RNA molecules while for the long single-stranded DNA molecules a smooth force-extension curve was observed. These experiments can be modeled by realizing that the mechanical response of a molecule in a given base-pairing pattern is determined by the mechanical properties of the m externally accessible bases in such a structure (see Fig. 4). Thus, if the base-pairing configurations are in equilibrium, all that is needed to model this system are the restricted partition functions Q_m of the base-pairing configurations which are summed over only those structures that have exactly m externally accessible bases and a polymer physics partition function $W_m(R)$ that describes a polymer of length m bases held at a fixed end-to-end distance R. The full partition function at end-to-end distance R is then the convolution

$$Z(R) = \sum_{m=0}^{N} Q_m W_m(R) \tag{3}$$

of these two quantities [64]. From this partition function all thermodynamic properties can be derived. Using this approach with the uniform pairing energy model with loop entropy yields a good description of the experiments on single-stranded DNA at least in the large force regime [63]. It is believed that the difference in the low force regime is due to counter ion and charge effects which can also be understood [67]. Calculating the partition functions Q_m with the realistic energy model and using appropriate polymer models for $W_m(R)$ yields quantitative agreement with the experiments on short RNA [64–66]. The most surprising outcome of applying these quantitative descriptions to more complicated RNA molecules is that the thermodynamic force-extension curve already becomes more or less featureless if the length of the RNA molecule is on the order of 200 bases due to a compensation effect between different structural elements [64]. Thus, there is no hope to determine the structure of an RNA molecule just by observing its mechanical response, as long as the system remains in thermodynamic equilibrium. As we will discuss below though, exploiting RNA kinetics gives much more information on the structure of an RNA molecule.

3 Non-equilibrium properties

3.1 Experimental data on DNA/RNA kinetics

Experiments that probe the base-pairing kinetics are challenging, and there has not been a systematic large-scale effort to dissect the kinetics to the same degree as has been done for the thermodynamics. Early relaxation experiments on bulk samples [68] already determined the rate for helix growth, i.e. the rate for closing a base-pair at the end of a helical segment, to be in the range $1 - 20 \times 10^6\, s^{-1}$. From reannealing experiments with periodic sequences, Pörschke [69] estimated the rate for the displacement of a bulge loop by one base to be roughly $5 \times 10^6\, s^{-1}$. This latter process amounts to the slippage of a base-pair, i.e. one base switches its binding partner. Hence, the most elementary steps in base-pairing kinetics occur on the (sub-)microsecond time scale.

Using modern optical single molecule methods, the closing of hairpin loops was found to be roughly 10 to 100 times slower [70]. The same methods were also used to study the dynamics of internal loops [71], yielding a surprisingly low estimate for the rate of helix growth ($10^4 - 10^5\, s^{-1}$), which may be an effect of the fluorophore tags. Very recently, the kinetics of spontaneous branch migration of Holliday junctions in DNA was examined [72]. Here, the lifetimes of the individual states were roughly in the millisecond to second time scale. More complicated rearrangements in the base-pairing pattern and the tertiary structure of RNA can be considerably slower and reach the time scale of minutes. Classical biochemical methods [73] and single molecule techniques, see e.g. [10, 74–77], complement each other in the study of the kinetics of RNA folding.

3.2 Theoretical and simulation approaches

While the thermodynamics of DNA/RNA base-pairing is fully determined by specifying a (free) energy for each base-pairing state, a full description of the kinetics in this state space requires the knowledge of all transition probabilities $W(n', t'|n, t)$ from state n at time t to state n' at time t'. In such a description, one does not explicitly consider the time evolution of the full spatial polymer configuration. Instead, the polymer dynamics enters only implicitly through the effective transition probabilities $W(n', t'|n, t)$ between different base-pairing states. Clearly, this simplification is necessary due to the enormous range of time scales in the dynamics of these molecules. Indeed, the rapid Brownian dynamics of the polymer degrees of freedom is usually well separated from the microsecond (and up) time scale of (significant) changes in the base-pairing state.

Commonly, the description is further simplified by assuming that the transitions between these states are simple Poisson processes, which are characterized by a single rate constant $k_{n\to n'}$ for each transition. The existing models differ in the set of states and transitions that are explicitly taken into account. While every kinetic model has to assure that each allowed state can indeed be reached from each initial condition (ergodicity), there are essentially two approaches that differ in the scale of the conformation changes that are allowed to take place in a single transition. One approach is to allow only single base steps, i.e. opening and closing of single base-pairs and slippage of a single bond [78–81]. Simulations using these kinetics are computer intensive and are usually practical only for relatively small molecules (e.g. on the order of 100 bases). This approach can also be appropriate when the base-pairing kinetics is coupled to another dynamical process that is externally driven, as in the example of translocation through a nanopore discussed below [81]. The other approach is to use larger scale rearrangements like helix formation and opening as the elementary steps [57, 61, 82, 83]. This approach, in particular in combination with the technique of exactly clustered stochastic simulation [61], can be used to study even the dynamics of large RNAs over long time scales. Note that whereas pseudo-knots are problematic to deal with in the recursion relation Eq. (2) of the equilibrium theory, pseudo-knots cause no specific problems in kinetic simulations [57, 61, 82, 83].

Besides choosing the set of elementary moves for a kinetic model, one must fix the associated kinetic rates. Of course, one has to assure that the kinetics reproduces the thermodynamics, if allowed to equilibrate. This is guaranteed when the rates satisfy detailed balance, which constrains the ratio of the forward and backward rate for a transition to the associated Boltzmann factor. The remaining rate constants must be estimated from the available experimental data on DNA/RNA kinetics, see above, since information on the detailed kinetic barriers for each elementary move is not available. As a result, the model kinetics is semi-quantitative at best (however, see Ref. [84], discussed below, for an example of a remarkably good agreement). This may appear as a drawback, and indeed, more detailed experimental information is highly desirable. On the other hand, the lack of a fully quantitative description does not impede the study of qualitative phenomena, some examples for which are discussed next.

3.3 Non-equilibrium phenomena

The non-equilibrium behavior of DNA and RNA is only beginning to be explored. To illustrate the types of phenomena that can emerge from the microscopic steps considered above, we discuss four examples here.

3.3.1 Dynamics of DNA slippage

Not only the thermodynamics, but also the kinetics of base-pairing can be probed through the application of forces on the piconewton scale. Let us consider a dsDNA with a periodic sequence, to which a shear force is applied on opposite strands at opposite ends, as indicated in Fig. 5. The base-pairing kinetics of this relatively simple system already displays a rich phenomenology [85]. From a physical point of view, periodic DNA is interesting, since periodic sequences have many non-native base-pairing conformations where one strand is shifted with respect to the other, and shearing probes the transitions between such states, i.e. the dynamics of DNA *slippage*. This is interesting also from a biological point of view, since DNA slippage during genome replication allows the expansion of nucleotide repeats, and, for certain repeats inside genes, triggers a variety of diseases including Huntington's disease. Note that the shear force is essential here, since the usual unzipping geometry, where the force is applied from the same end of the dsDNA, probes only the consecutive opening of *native* base-pairs, i.e. those present in the ground state of the molecule.

Many years ago, Pörschke melted periodic dsDNA and studied the kinetics of reannealing through UV absorption [69]. Based on these experiments, he already suggested the mechanism that permits DNA slippage: small bulge loops can form at the ends of the molecule when a few bases spontaneously unbind and rebind shifted by one or several repeat units. Once formed, a bulge loop may diffuse along the molecule and anneal at the other end, effectively sliding the two strands against each other by a length equal to the size of the bulge loop, see Fig. 5. This mechanism involves only small energetic barriers compared to the large barrier for complete unbinding and reassociation.

An applied shear force can induce DNA slippage [85]. At zero force, the rates for bulge loop creation are the same at all four strand ends, if the two single strands are perfectly aligned. Two misaligned strands have imbalanced rates which tend to realign them. As a consequence, a certain force threshold f_c needs to be overcome in order to produce a net outward drift separating the two strands. This critical force can be estimated by balancing the binding energy per base-pair, $\varepsilon_{\rm b}$, with the mechanical work exerted when a base-pair of length $\ell_{\rm d}$ is converted into two single-stranded bases of length $\ell_{\rm s}$, yielding $f_c \approx \varepsilon_{\rm b}/(2\ell_{\rm s} - \ell_{\rm d})$. Fig. 5 displays the scaling of the

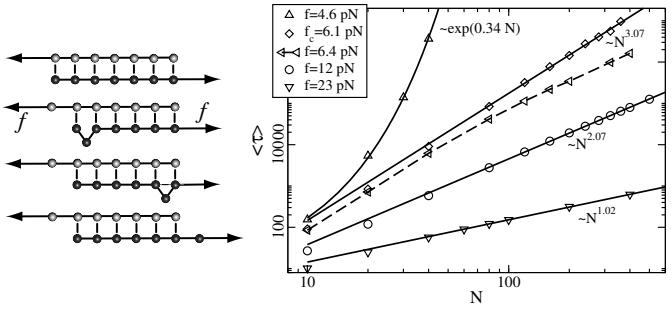

Fig. 5. Dynamics of DNA slippage under tension. Left: In periodic DNA sequences, sliding is mediated by bulge loops that diffuse along the DNA. When a bulge loop reaches the opposite end, the two strands have effectively slipped against each other by a distance equal to the loop size. Right: Scaling of the mean rupture time with the number of bases N for different shear forces, with DNA parameters roughly corresponding to AT-sequences at $50°C$. The symbols represent Monte Carlo data, while the solid lines for $f \geq f_c$ are power law fits. For $f < f_c$ the rupture time increases exponentially. The data for f slightly larger than f_c (connected by the dashed line), demonstrates the crossover from diffusive to drift behavior, and shows that the cubic scaling indeed holds only at the critical force.

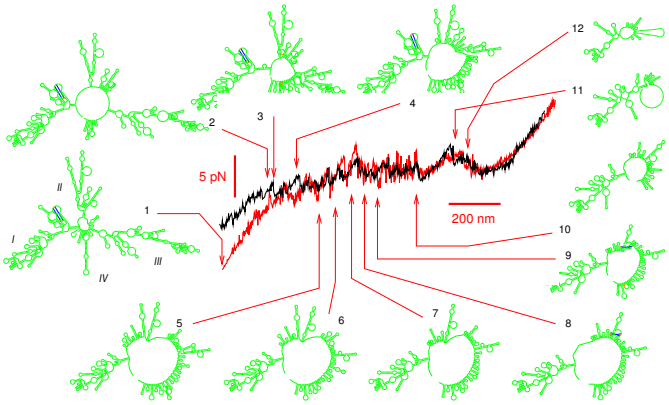

Fig. 6. Comparison between an experimental force-extension curve (black) for the 16S ribosomal RNA of *E. coli* and a model simulation (red), together with some structures (green) along the computed unfolding pathway. Taken (with permission) from Ref. [84].

mean rupture time (time until complete separation of the two strands) with the number of bases N for a number of different forces (see Ref. [85] for the detailed model description and the parameter choice). There are four distinct asymptotic behaviors: an exponential increase with N for small forces, a cubic scaling with N at f_c, a nearly quadratic scaling above f_c but below a second threshold f^*, and linear scaling above f^*. The behavior in the two extremes is easily interpreted: for small f, rupture is driven by thermal fluctuations across a large free energy barrier with an associated Kramers time that scales exponentially with N, and linear scaling at large f is expected when individual bonds break sequentially at a constant rate.

The rupture dynamics at the critical force is best understood by analogy with the reptation problem [86], since bulge loops in the DNA structure behave similarly to the "stored length" excitations of a single chain in a polymer network: these excitations are generated at the ends of the polymer with a constant rate, diffuse along the polymer and reach the other end with a probability $\sim N^{-1}$. Therefore, the macroscopic diffusion constant for the relative motion of the two DNA strands scales as $D \sim N^{-1}$ and the time for diffusion over distance N is $\sim N^3$. For $f > f_c$ strand separation is energetically a downhill process, which induces a drift velocity v between the two strands, leading to a quadratic scaling of the mean rupture time. However, this behavior does not persist for large forces, due to a change in the rupture *mode*: at forces larger than $f^* \approx \varepsilon_b/(\ell_s - \ell_d)$ the double strand can open by *unraveling* from both ends, leading to a rupture time that scales linearly with N.

The bulge loop dynamics in periodic DNA is a many-particle problem with both 'particles' and 'antiparticles', since bulge loops on opposite strands annihilate each other when they overlap. Similarly, there is pair creation, and a residual interaction also among the particles of each class. The collective properties emerging from these interactions have only begun to be analyzed [85]. We believe this example illustrates that the dynamics of DNA/RNA has some appealing connections to other areas of physics.

3.3.2 Force-induced denaturation of RNA

In Section 2.3.3 we already discussed the stretching of an RNA molecule from both ends in the adiabatic limit, where the extension of the molecule is increased so slowly that the secondary structure remains in quasi-equilibrium during the process. When the extension is increased more rapidly, the force-extension curve reflects the structural dynamics of the RNA [66, 84]. Ref. [84] has compared experimental force-extension traces with stochastic simulations that use the opening and closing of complete helices as elementary steps. The authors found a remarkably good agreement as shown in Fig. 6 taken from Ref. [84]. With the help of their simulations, the authors examined the unfolding pathway and noted that it does not only consist of the successive opening of native helices, but that long-lived intermediates with non-native helices have a significant effect on the force-extension traces. This forced unfolding therefore demonstrates, on a single-molecule level, the presence of kinetic traps due to non-native secondary structure, which is known to hamper also the inverse, folding process [73].

In this case, the coarse-grained kinetic model is apparently adequate, which is presumably due to the fact that only large scale rearrangements are visible in the observed force extension curves. These large scale rearrangements are dominated by the thermodynamic free energy barriers associated with the opening of entire helices.

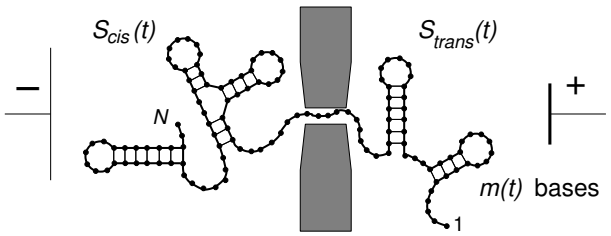

Fig. 7. Driven translocation of a structured RNA molecule through a tiny pore, which allows single but not double strand to pass. Individual DNA or RNA molecules are driven through this hole by an electric field using the fact that nucleic acids are positively charged. By observing the ion current through the pore, it can be determined if a molecule is in the pore or not. Thus, the translocation time for individual molecules can be measured.

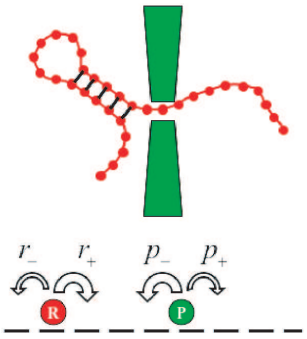

Fig. 8. Two random walker model for translocation of an RNA molecule through a pore. The two random walkers represent the position of the molecule with respect to the pore (P), and the position of the first closed base-pair before the pore (R). The dynamics of translocation results from the two walkers being biased in opposing directions.

3.3.3 Co-transcriptional RNA folding

It is known that RNA folding can be very slow when studied *in vitro*, yet the same molecule may quickly fold *in vivo* [73]. One of the mechanisms that can lead to this difference is co-transcriptional folding: whereas *in vitro*, folding is induced by a change in ambient conditions (e.g. a sudden decrease in temperature), RNA folding *in vivo* is concurrent with RNA synthesis. This effect was strikingly demonstrated in Ref. [57] with kinetic folding simulations of the HDV ribozyme, a well-studied enzymatic RNA. The kinetic model was the same as in the preceding section. The authors found that simulations starting with the entire sequence and no base-pairs, resulted in about 2/3 of the runs being trapped in a misfolded intermediate for up to a minute of estimated real time. From a biological point of view this is very surprising since the replication of HDV's genome takes only about $30s$. The apparent contradiction between replication time and folding time was resolved when folding was simulated concurrently with synthesis at a rate of 50 bases per second: under these conditions the fraction of kinetically trapped ribozyme structures decreased to less than 10 %.

3.3.4 Dynamics of translocation through nanopores

During transcription, the dynamic processes of RNA synthesis and base-pairing are coupled. In contrast, during *translation* the base-pairing dynamics is coupled to the *translocation* of the RNA through a tiny opening in the ribosome. A similar translocation scenario is studied in a series of recent single-molecule experiments reviewed in [87], which use electric fields to drive RNA and DNA through tiny pores that let single but not double strands pass. Initially, these experiments mainly characterized the translocation of homopolymers, whereas the effect of base-pairing on translocation, see Fig. 7, is now beginning to be explored [11, 88–90].

Without base-pairing, translocation of (not too long) RNAs can be described as a one-dimensional drift-diffusion process [91], with the number of translocated bases, $m(t)$, as the reaction coordinate, see Fig. 7. In general, the coupling to the base-pairing dynamics destroys this simple picture [81]. However, some insight can be gained by considering the adiabatic limit where the internal base-pairing dynamics of the RNA is assumed to be much faster than the translocation process. In this limit, the dynamics is again one-dimensional, however with sequence-dependent kinetic barriers. These barriers are much smaller than one may naively expect: for instance, the barrier for translocation of a single long hairpin is not the total binding free energy of the hairpin, but is substantially reduced through the formation of non-native base-pairs, e.g. among the bases that have already translocated. The most significant barrier turns out to be the "entrance" of the pore into the structure.

The qualitative effect that non-native base-pairs can contribute to a significant speed up in translocation remains operative even outside the adiabatic (slow translocation) limit. In the opposite limit, the base-pairing rate caps the translocation speed. The basic physics of the crossover between these two limits can be understood with the help of a very simple model, see Fig. 8: The pore is represented by a random walker with a bias (due to the external voltage) to run into the RNA structure, whereas the index of the first closed base-pair in front of the pore is another random walker with a bias in the opposite direction (due to the binding free energy of base-pairs). This stochastic "push-of-war" leads to an average drift in one direction and determines the translocation speed [81].

Besides an electrical field there are other possible driving forces for translocation. Among these, mechanical pulling is particularly interesting, because these techniques allow not only the application of a force, but simultaneously the measurement of an extension. Ref. [92] argues that with this additional information, the base-pairing pattern of an RNA molecule (including pseudo-knots) can in principle be determined, if its sequence is already known.

4 Conclusions and Outlook

Base pairing in nucleic acids is conceptionally very simple. Yet, as they are applied to molecules of even moderate length, the simple rules of base-pairing lead to a variety of interesting emergent physical phenomena. Nature not only has to respect the emergent physical properties of base-pairing but in many cases actually exploits them. In addition, human engineers also start to control and make use of the interesting physical properties of base-pairing [93]. This makes it important to obtain a fundamental understanding of the physics of base-pairing.

Here, we have shown how some of the phenomena resulting from the simple base-pairing rules can be understood based on theoretical models. However, some of these approaches are only a first step. While the thermodynamics of base-pairing is by now a relatively mature field, the kinetics of base-pairing is only beginning to be understood and there are certainly many surprises awaiting researchers that are trying to uncover how base-pairing kinetics affects biological phenomena and engineering applications.

Acknowledgements

Our view of the biophysics of base pairing in DNA and RNA summarized in this article has been shaped by numerous discussions and collaborations, for which we are very grateful. Since the number of individuals we interacted with on these topics is too large to list all names, we will make only one special acknowledgement to the person who introduced both of us to the subject of DNA and RNA biophysics and has been a collaborator on many of the works presented here, Terence Hwa.

References

1. B. Alberts, D. Bray, J. Lewis, M. Raff, K. Roberts, and J. D. Watson, *Molecular Biology of the Cell*, (Garland, 2002)
2. J. Couzin, Science **298**, 2296 (2002)
3. T. Cech, Biosci. Rep. **10**, 239 (1990)
4. M. Morita, Y. Tanaka, T. Kodama, Y. Kyogoku, H. Yanagi, and T. Yura, Genes Dev. **13**, 655 (1999)
5. R. Poot, N. Tsareva, I. Boni, and J. van Duin, Proc. Natl. Acad. Sci. USA **94**, 10110 (1997)
6. J. H. Nagel and C. W. Pleij, Biochimie **84**, 913 (2002)
7. R. Micura and C. Höbartner, ChemBioChem **4**, 984 (2003)
8. I. Tinoco and C. Bustamante, J. Mol. Biol. **293**, 271 (1999)
9. U. Bockelmann, B. Essevaz-Roulet, and F. Heslot, Phys. Rev. E **58**, 2386 (1998)
10. J. Liphardt, B. Onoa, S. B. Smith, J. Tinoco, Ignacio, and C. Bustamante, Science **292**, 733 (2001)
11. J. Mathe, H. Visram, V. Viasnoff, Y. Rabin, and A. Meller, Biophys. J. **87**, 3205 (2004)
12. J. SantaLucia, Jr., Proc. Natl. Acad. Sci. USA **95**, 1460 (1998)
13. S. Freier, R. Kierzek, J. Jaeger, N. Sugimoto, M. Caruthers, T. Neilson, and D. Turner, Proc. Natl. Acad. Sci. USA **83**, 9373 (1986)
14. D. Poland and H. Scheraga, J. Chem. Phys. **45**, 1456 (1966)
15. M. E. Fisher, J. Chem. Phys. **45**, 1469 (2000)
16. Y. Kafri, D. Mukamel, and L. Peliti, Phys. Rev. Lett. **85**, 4988 (2000)
17. D. Mathews, J. Sabina, M. Zuker, and D. Turner, J. Mol. Biol. **288**, 911 (1999)
18. B. Zimm and J. Bragg, J. Chem. Phys. **28**, 1246 (1958)
19. N. Mermin and H. Wagner, Phys. Rev. Lett. **17** (1966)
20. B. Zimm, J. Chem. Phys. **33**, 1349 (1960)
21. M. Peyrard and A. Bishop, Phys. Rev. Lett. **62**, 2755 (1989)
22. N. Theodorakopoulos, T. Dauxois, and M. Peyrard, Phys. Rev. Lett. **85**, 6 (2000)
23. E. Carlon, E. Orlandini, and A. Stella, Phys. Rev. Lett. **88**, 198101 (2002)
24. M. Causo, B. Coluzzi, and P. Grassberger, Physica A - Stat. Mech. Appl. **314**, 607 (2002)
25. A. Hanke and R. Metzler, Phys. Rev. Lett. **90**, 159801 (2003)
26. Y. Kafri, D. Mukamel, and L. Peliti, Phys. Rev. Lett. **90**, 159802 (2003)
27. M. Azbel, Physica A - Stat. Mech. Appl. **321**, 571 (2003)
28. L.-H. Tang and H. Chaté, Phys. Rev. Lett. **86**, 830 (2001)
29. D. Cule and T. Hwa, Phys. Rev. Lett. **79**, 2375 (1997)
30. A. Campa and A. Giansanti, Phys. Rev. E **58**, 3585 (1998)
31. R. Blake, J. Bizzaro, J. Blake, G. Day, S. Delcourt, J. Knowles, K. Marx, and J. SantaLucia, Jr., Bioinformatics **15**, 370 (1999)
32. R. Blossey and E. Carlon, Phys. Rev. E **68**, 061911 (2003)
33. T. Garel and H. Orland, Biopolymers **75**, 453 (2004)
34. S. Ares, N. Voulgarakis, K. Rasmussen, and A. Bishop, Phys. Rev. Lett. **94**, 035504 (2005)
35. P. de Gennes, Biopolymers **6**, 715 (1968)
36. M. Waterman *Advan. in Math. Suppl. Studies*, (Academic Press, New York, 1978) Vol. 1, pp. 167–212
37. R. Nussinov and A. Jacobson, Proc. Natl. Acad. Sci. USA **77**, 6309 (1980)
38. P. G. Higgs, Quart. Rev. Biophys. **33**, 199 (2000)
39. J. McCaskill, Biopolymers **29**, 1105 (1990)
40. M. Zuker, Nucleic Acids Res. **31**, 3406 (2003)
41. I. L. Hofacker, W. Fontana, P. F. Stadler, L. Bonhoeffer, M. Tacker, and P. Schuster, Monatshefte f. Chemie **125**, 167 (1994)
42. Y. Ding, C. Chan, and C. Lawrence, Nucleic Acids Res. **32**, W135 (2004)
43. P. G. Higgs, Phys. Rev. Lett. **76**, 704 (1996)
44. S.-J. Chen and K. A. Dill, Proc. Natl. Acad. Sci. USA **97**, 646 (2000)

45. A. Pagnani, G. Parisi, and F. Ricci-Tersenghi, Phys. Rev. Lett. **84**, 2026 (2000)
46. A. K. Hartmann, Phys. Rev. Lett. **86**, 1382 (2001)
47. A. Pagnani, G. Parisi, and F. Ricci-Tersenghi, Phys. Rev. Lett. **86**, 1383 (2001)
48. F. Krzakala, M. Mézard, and M. Müller, Europhys. Lett. **57**, 752 (2002)
49. E. Marinari, A. Pagnani, and F. Ricci-Tersenghi, Phys. Rev. E **65**, 041919 (2002)
50. R. Bundschuh and T. Hwa, Europhys. Lett. **59**, 903 (2002)
51. R. Bundschuh and T. Hwa, Phys. Rev. E **65**, 031903 (2002)
52. M. Müller, Phys. Rev. E **67**, 021914 (2003)
53. V. S. Pande, A. Y. Grosberg, and T. Tanaka, Rev. Mod. Phys. **72**, 259 (2000)
54. R. Bundschuh and T. Hwa, Phys. Rev. Lett. **83**, 1479 (1999)
55. D. Moroz and T. Hwa, to be published
56. E. Rivas and S. Eddy, J. Mol. Biol. **285**, 2053 (1999)
57. H. Isambert and E. D. Siggia, Proc. Natl. Acad. Sci. USA **97**, 6515 (2000)
58. H. Orland and A. Zee, Nucl. Phys. B **620**, 456 (2002)
59. A. Kabakçioglu and A. Stella, Phys. Rev. E **70**, 011802 (2004)
60. R. Lyngsø and C. Pedersen, J. Comp. Biol. **7**, 409 (2000)
61. A. Xayaphoummine, T. Bucher, and H. Isambert, Proc. Natl. Acad. Sci. USA **100**, 15310 (2003)
62. B. Maier, D. Bensimon, and V. Croquette, Proc. Natl. Acad. Sci. USA **97**, 12002 (2000)
63. A. Montanari and M. Mézard, Phys. Rev. Lett. **86**, 2178 (2005)
64. U. Gerland, R. Bundschuh, and T. Hwa, Biophys. J. **81**, 1324 (2001)
65. S. Cocco, J. Marko, R. Monasson, A. Sarkar, and J. Yan, Eur. Phys. J. E **10**, 249 (2003)
66. M. Manosas and F. Ritort, Biophys. J. **88**, 3224 (2000)
67. M.-N. Dessinges, B. Maier, Y. Zhang, M. Peliti, D. Bensimon, and V. Croquette, Phys. Rev. Lett. **89**, 248102 (2002)
68. M. Craig, D. Crothers, and P. Doty, J. Mol. Biol. **62**, 383 (1971)
69. D. Pörschke, Biophys. Chem. **2**, 83 (1974)
70. G. Bonnet, O. Krichevsky, and A. Libchaber, Proc. Natl. Acad. Sci. USA **95**, 8602 (1998)
71. G. Altan-Bonnet, A. Libchaber, and O. Krichevsky, Phys. Rev. Lett. **90**, 138101 (2003)
72. S. McKinney, A. Freeman, D. Lilley, and T. Ha, Proc. Natl. Acad. Sci. USA **102**, 5715 (2005)
73. D. Thirumalai and S. A. Woodson, RNA **6**, 790 (2000)
74. X. Zhuang, L. E. Bartley, H. P. Babcock, R. Russell, T. Ha, D. Herschlag, and S. Chu, Science **288**, 2048 (2000)
75. X. Zhuang, H. Kim, M. J. B. Pereira, H. P. Babcock, N. G. Walter, and S. Chu, Science **296**, 1473 (2002)
76. B. Onoa, S. Dumont, J. Liphardt, S. B. Smith, J. Tinoco, Ignacio, and C. Bustamante, Science **299**, 1892 (2003)
77. X. Zhuang, Annu. Rev. Biophys. Biomol. Struct. **34**, 399 (2005)
78. C. Flamm, W. Fontana, I. L. Hofacker, and P. Schuster, RNA **6**, 325 (2000)
79. W. Zhang and S.-J. Chen, Proc. Natl. Acad. Sci. USA **99**, 1931 (2002)
80. S. Cocco, J. Marko, and R. Monasson, Eur. Phys. J. E **10**, 153 (2003)
81. R. Bundschuh and U. Gerland, (2005) Coupled dynamics of RNA folding and nanopore translocation, q-bio/0508004
82. A. Gultyaev, F. van Batenburg, and C. Pleij, Nucleic Acids Res. **23**, 3718 (1995)
83. A. Xayaphoummine, T. Bucher, F. Thalmann, and H. Isambert, Nucleic Acids Res. **33**, W605 (2005)
84. S. Harlepp, T. Marchal, J. Robert, J.-F. Leger, A. Xayaphoummine, H. Isambert, and D. Chatenay, Eur. Phys. J. E **12**, 605 (2003)
85. R. A. Neher and U. Gerland, Phys. Rev. Lett. **93**, 198102 (2004)
86. P.-G. de Gennes, J. Chem. Phys. **55**, 572 (1971)
87. A. Meller, J. Physics: Condensed Matter **15**, R581 (2003)
88. W. Vercoutere, S. Winters-Hilt, H. Olsen, D. Deamer, D. Haussler, and M. Akeson, Nat. Biotechnol. **19**, 248 (2001)
89. A. F. Sauer-Budge, J. A. Nyamwanda, D. K. Lubensky, and D. Branton, Phys. Rev. Lett. **90**, 238101 (2003)
90. J. Mathe, A. Arinstein, Y. Rabin, and A. Meller, Europhys. Lett. **73**, 128 (2006)
91. D. K. Lubensky and D. R. Nelson, Biophys. J. **77**, 1824 (1999)
92. U. Gerland, R. Bundschuh, and T. Hwa, Phys. Biol. **1**, 19 (2004)
93. N. C. Seeman, Nature **421**, 427 (2003)